NOVEL HINGING MOTION OBSERVED IN LARGE, CYCLIC MOLECULES: SYNTHESIS AND CHARACTERIZATION

By

Joey Mellberg

Submitted in partial fulfillment of

the requirements for Departmental Honors in the Department

of Chemistry and Biochemistry

Texas Christian University

Fort Worth, Texas

May 8, 2023

NOVEL HINGING MOTION OBSERVED IN LARGE, CYCLIC MOLECULES: SYNTHESIS AND CHARACTERIZATION

Project Approved:

Supervising Professor: Eric Simanek, Ph.D.

Department of Chemistry and Biochemistry

David Minter, Ph.D.

Department of Chemistry and Biochemistry

Mikaela Stewart, Ph.D.

Department of Biology

ABSTRACT

This research aims to understand how to design and control molecular hinges. The molecular hinges of interest are nano-sized equivalents of door hinges. Such hinges could find applications in new materials or the design of new drugs.

The foundation for this research was the observation that a large, ring-shaped molecule - a so-called macrocycle - prepared by a colleague folded and unfolded rapidly at room temperature. Two research questions arose from this observation: was the hinge behavior unique to this molecule, and could the hinging rate be controlled?

Addressing these questions required the three-step synthesis of a related macrocycle. This new molecule had groups equivalent to putting grit around the hinge's pin. The difference in the rate of hinging motion due to the addition of these groups was observed using a technique called variable temperature NMR spectroscopy.

The results of this work revealed that hinging is a general phenomenon for some of these macrocycles. Second, the 'molecular dirt' designed into this new hinge reduced the rate of hinge motion from 2000 times per second to 20 times per second.

This work is currently undergoing revisions for *Chemistry* based on the novelty of this molecular device and the scientific community's interest in molecular machines.

INTRODUCTION

Most molecules exhibit random movement when in solution, but the scientific community's interest in molecular machines has led to the exploration of molecules that mimic machines in everyday life including gears,[1] pumps,[2,3] and tweezers.[4]

The 2016 Nobel Prize in Chemistry was split between three chemists: Sauvage, Stoddart, and Feringa, "for the design and synthesis of molecular machines." Jean-Pierre Sauvage of the University of Strasbourg (France) was responsible for synthesizing a chain-like structure called a catenane.[5] These catenanes are synthesized using a metal ion that acts as a template. In the first strategy, "entwining," two halves of a chain are wrapped around each other and then closed by two additional half links. In the second strategy, "gathering and threading," a half link is threaded through a full link, then the half link is closed by adding another half. This principle can be extended into the synthesis of molecular muscles, which can expand and contract depending on the ion chelated to the molecule, as illustrated in **Figure 1**.

---

[1] Gisbert, Y.; Abid, S.; Kammerer, C.; Rapenne, G. Molecular Gears: From Solution to Surfaces. Chemistry. *Chem. Eur. J.*, **2021**, *27*, 12019-12031.
[2]Amano, S.; Fielden, S. D. P.; Leigh, D. A. A catalysis-driven artificial molecular pump. *Nature* **2021**, *594*, 529-534.
[3] Sabatino, A.; Penocchio, E.; Ragazzon, G.; Credi, A.; Frezzato, D. Individual-Molecule Perspective Analysis of Chemical Reaction Networks: The Case of a Light-Driven Supramolecular Pump. *Angew. Chem. Int. Ed.* **2019**, *58* 14341-14348.
[4] Muraoka, R.; Kinbara, K.; Aida, T. Mechanical twisting of a guest by a photoresponsive host. *Nature* **2006**, *440*, 512-515.
[5] Jean-Pierre Sauvage – Nobel Lecture. NobelPrize.org. Nobel Prize Outreach AB 2023. Thu. 23 Mar 2023. <https://www.nobelprize.org/prizes/chemistry/2016/sauvage/lecture/>

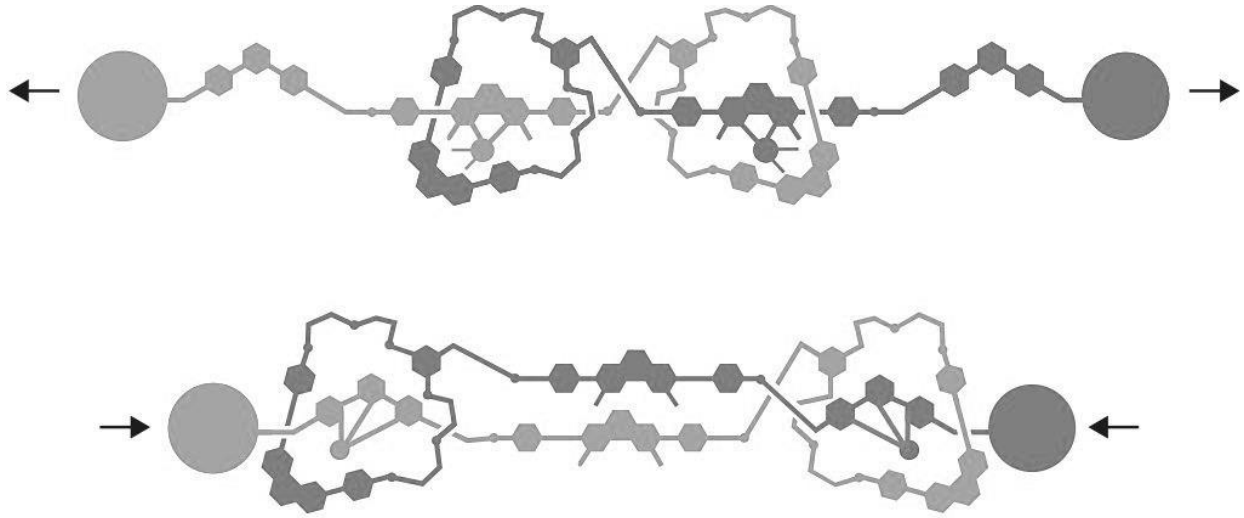

Figure 1. Shows the contraction and expansion of the molecular muscle synthesized by Dr. Sauvage[1]. Figure adapted from The Royal Swedish Academy of Sciences.

Sir J. Frasier Stoddart of Northwestern University (US) synthesized an axle-like structure called a rotaxane. It consists of two parts: a dumbbell-shaped molecule and a ringed structure. These structures can be used as molecular switches where the ring can move between one side of the dumbbell and the other about 1000 times per second in acetone.[6] Dr. Stoddart also synthesized a molecule that can move the ring from the left to the right of the dumbbell by modulating the pH. Nevertheless, other molecules synthesized by Dr. Stoddart can act as switches in molecular electronics and stoppers in nanovalves.

[6] Sir J. Fraser Stoddart – Nobel Lecture. NobelPrize.org. Nobel Prize Outreach AB 2023. Thu. 23 Mar 2023. <https://www.nobelprize.org/prizes/chemistry/2016/stoddart/lecture/>

Bernard Feringa of the University of Groningen (Germany) synthesized a molecular motor that would continuously spin in the same direction.[7] This motor was powered by light and temperature and could spin, as shown in **Figure 2**.

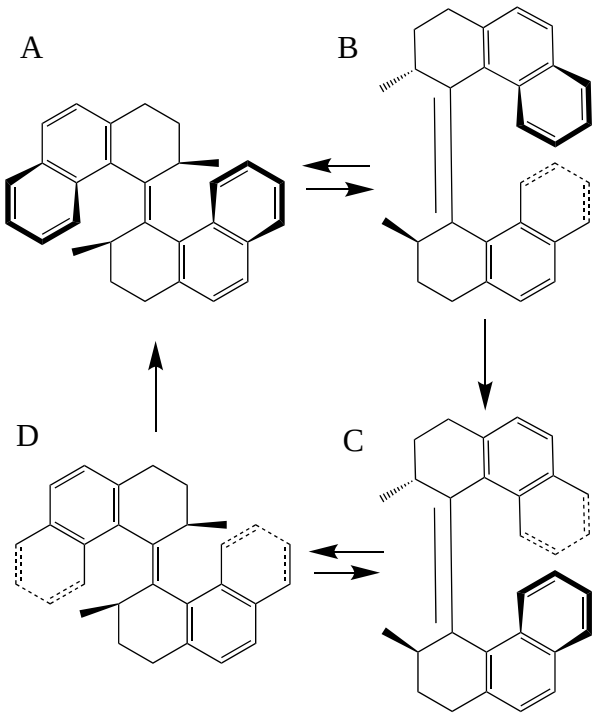

Figure 2. Professor Feringa's motor cycles through conformation A to B and C to D using light at a specific wavelength and between conformation B to C and D to A using heat.

Another example of an everyday object with a molecular relative is a butt hinge, known for its use as a door hinge (**Figure 3**)**.** A door hinge comprises of two leaves and a hinge pin. In this arrangement, the leaves are responsible for fastening the door and the door frame to the hinge, while the hinge pin provides an axis of rotation around which two leaves move to demonstrate the classic hinging motion.

[7] Bernard L. Feringa – Nobel Lecture. NobelPrize.org. Nobel Prize Outreach AB 2023. Wed. 12 Apr 2023. <https://www.nobelprize.org/prizes/chemistry/2016/feringa/lecture/>

Figure 3. A classic butt hinge containing two flat domains (leaves) and the hinge pin. The hinge rotates from conformation A to C through conformation B.

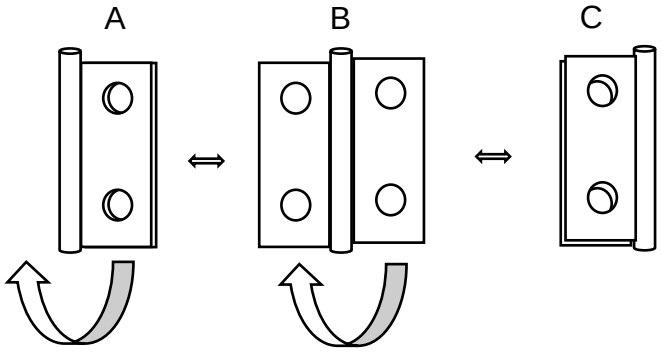

Only a few molecules display this unique hinging motion including the large, ring-shaped molecule (referred to hereafter as a macrocycle) that is described here. Like a door hinge, the molecular hinge has flat leaves and the molecular equivalent of pins and knuckles (Chart 1). Earlier studies revealed that hinge motion was fast when the hinge domain incorporated the amino acid glycine.[8] The goals of this research were 1) to determine whether hinge motion was a general phenomenon with these macrocycles and 2) to attempt to exert control over hinge motion.

To accomplish these ends, glycine was replaced with 2-aminoisobutyric acid (AIB) residues. The result is that the small hydrogen atoms of glycine are replaced with large methyl groups of AIB. Here, we report that an **AIB-AIB** macrocycle was successfully synthesized, and its motion was subsequently characterized using nuclear magnetic resonance (NMR) spectroscopy. The AIB-AIB macrocycle also exhibits hinging motion when in solution,[9] but at a slower rate than the glycine-glycine macrocycle (G-G). The

[8] Riccardo Capelli, Alexander J. Menke, Hongjun Pan, Benjamin G. Janesko, Eric E. Simanek, and Giovanni M. Pavan. *ACS Omega* **2022** *7* (34), 30291-30296
DOI: 10.1021/acsomega.2c03536
[9] Alexander J. Menke, Joseph M. Mellberg, Hongjun Pan, Joseph H. Reibenspies, Benjamin G. Janesko, and Eric E. Simanek.

molecule was observed moving from conformation **A** to **B**, to **C**, before returning to conformation **A** via intermediate **B,** as depicted in **Figure 3**.

RESULTS AND DISCUSSION

*Synthesis of the **Acid**.* The synthetic route used for **AIB-AIB** is shown in Scheme 1. The **AIB-AIB** macrocycle was achieved using an efficient, three-step synthesis. In the first step, BOC-hydrazine, AIB, and dimethylamine (DMA) were added to cyanuric chloride in a stepwise fashion to yield the acid intermediate. This reaction is highly selective because each addition reduces the reactivity of the triazine ring. The **Acid** was purified using silica gel exchange chromatography using a mixture of dichloromethane and methanol as the eluent.

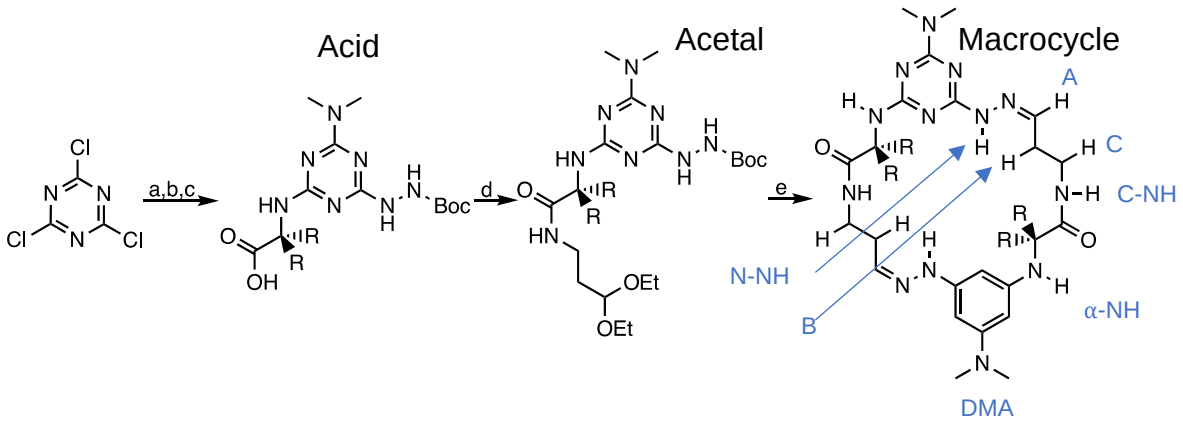

Scheme 1. Synthesis of **G-G** (Hinge 1, R = H) and **AIB-AIB** (Hinge 2, R = Me). ^{1}H assignments are noted in blue. a) t-butyl carbazate, -10^{o} C, THF, dropwise, 4.5 hours. b) 2-Aminoisobutyric Acid (AIB), THF, dropwise, 2 hours. c) Dimethylamine, THF, overnight. d) HOBT, HBTU, DIPEA, 3,3-diethoxypropylamine, DMF, overnight. e) 1:1 DCM:TFA, evaporate until dry.

^{1}H and ^{13}C NMR spectroscopy were performed to establish that the **Acid** was synthesized. NMR leverages a quantum mechanical principle called spin and a powerful electromagnet. All electrons are either spin up or down, and by applying a magnetic field, the magnet causes the electron spin to fluctuate, which allows a machine to differentiate

between different environments for a given nucleus. Scientists can analyze this information (called a spectrum) and determine the molecule's structure in solution using this technique. In our case, this technique can verify that the target molecule has been

successfully synthesized. Here, the NMR in **Figure 4** clearly shows evidence for all three additions. First, the presence of M1 and M2 shows that DMA was successfully added. Second, the presence of the BOC group on the spectrum suggests that this addition occurred successfully too. Finally, the β-methyl peaks suggest that **AIB** was

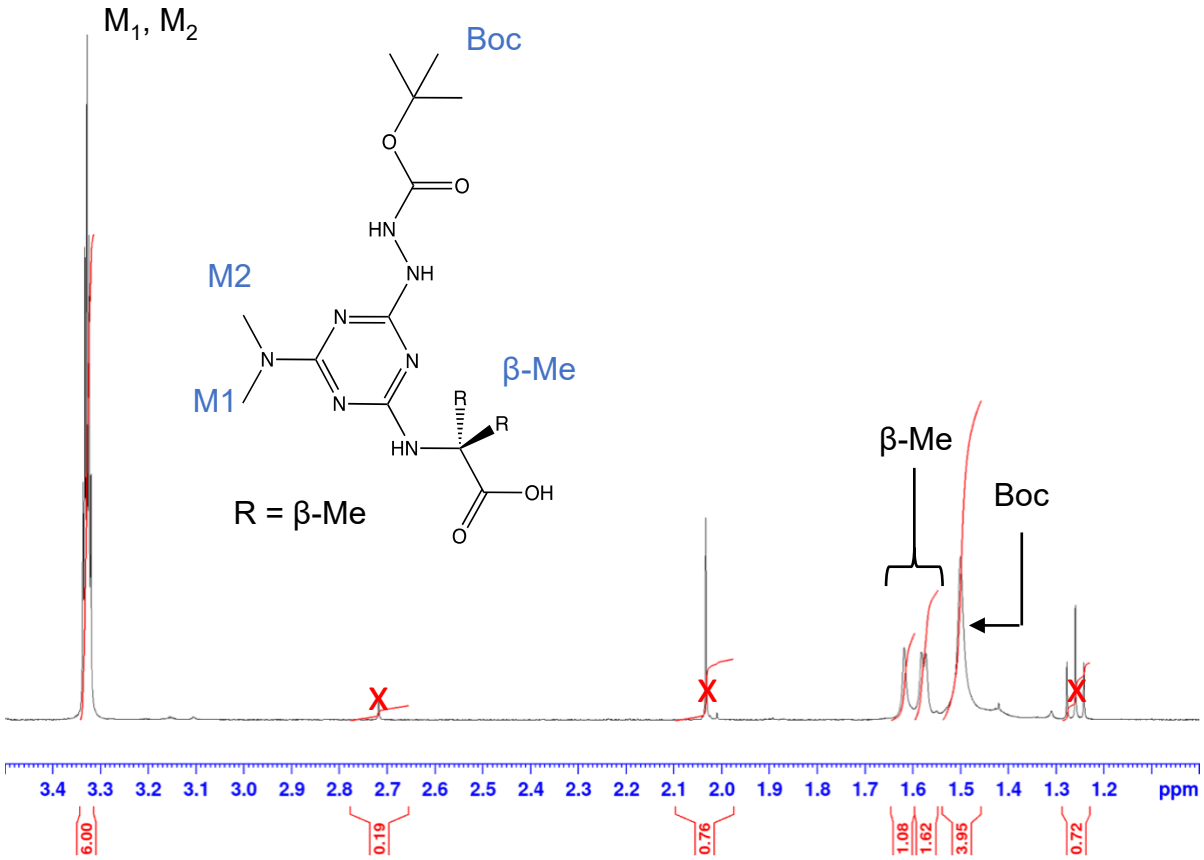

Figure 4. ^{1}H NMR Spectrum of the **ACID** taken in $CDCl_3$. The blue labels denote the protons on the **ACID** and the black labels denote which resonances in the ^{1}H NMR spectrum that correspond to those protons.

successfully substituted onto the molecule, which completes the structure.

The ^{13}C spectrum is shown in **Figure 5**, corroborating the ^{1}H NMR. In this spectrum, the presence of the acid C=O, BOC C=O, M1, and M2 show that **AIB**, BOC, and DMA were successfully added to this molecule, thereby confirming the findings from the ^{1}H NMR spectrum.

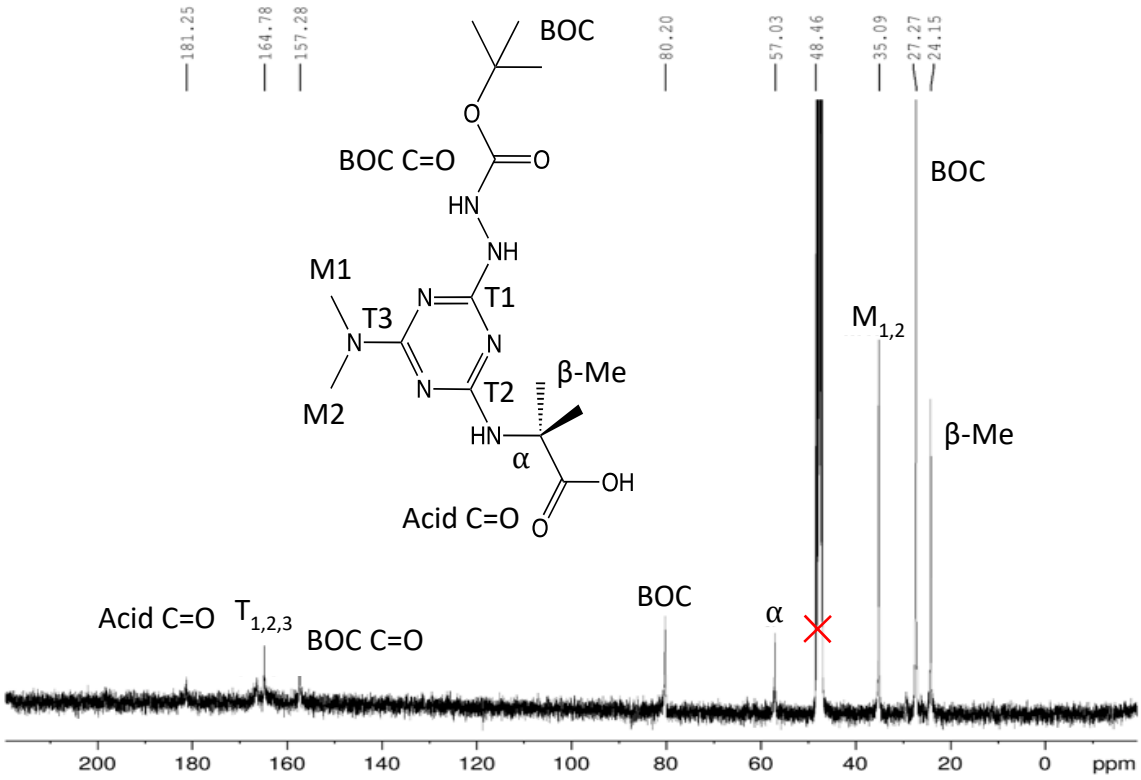

Figure 5. The ^{13}C NMR spectrum in MeOD? shows the expected number of peaks and is overall consistent with the structure of the acid intermediate. The red "X" is from the NMR solvent.

*Synthesis of the **Monomer**.* In the second step of the reaction sequence, 1-amino-3,3-diethoxypropane was added to the **Acid** to obtain the **monomer**. The reaction is monitored by TLC (thin-layer chromatography) to track the conversion of the **Acid** and acetal reactants to the final **Monomer** product. Thin layer chromatography is similar in that it uses silica to separate molecules as the eluent moves but different in that the silica is fixed to a small pane of glass, and the amount of product used is considerably

lower. The transition of two spots by TLC to a single spot at a different position on the TLC plate indicates that this reaction has occurred. After the reaction was complete, as indicated by TLC, silica gel exchange chromatography was used to purify the product.

The ^{1}H NMR spectrum of the monomer is shown in **Figure 6**. The acetal methyl and methylene proton peaks at 1.18 and 3.5 ppm, respectively, suggest that the acetal linker

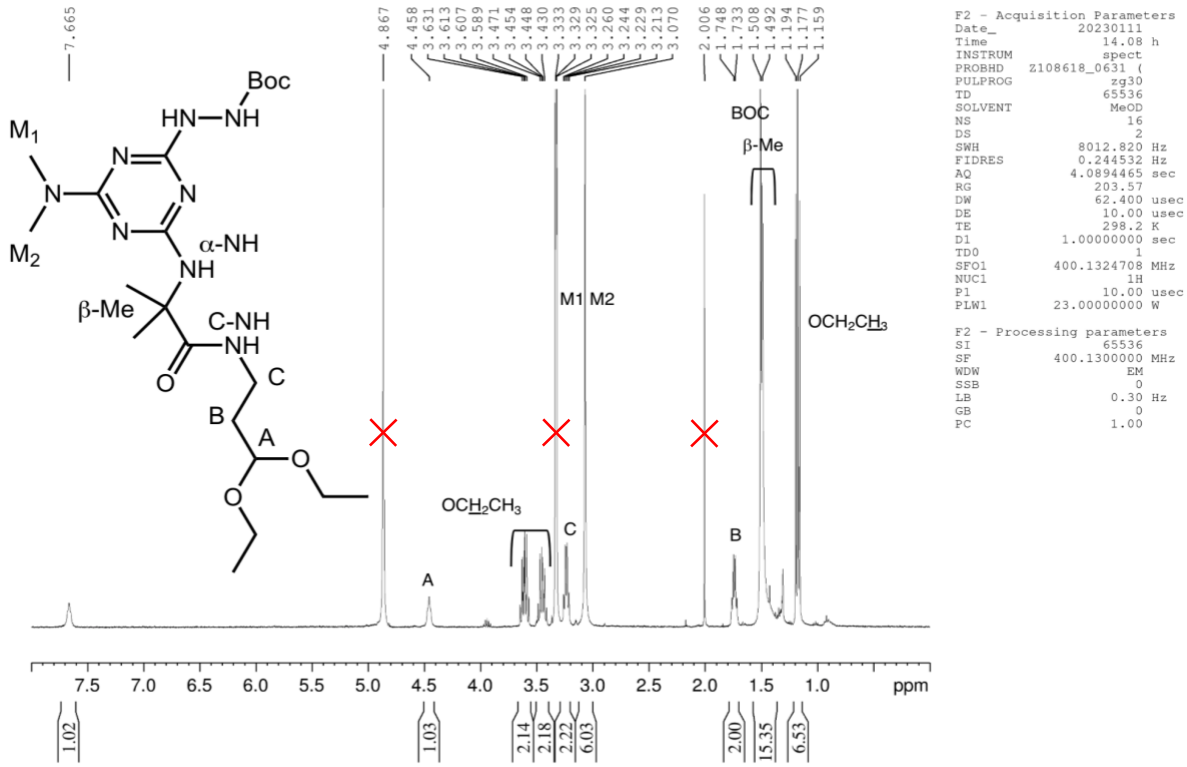

Figure 6. ^{1}H NMR spectrum of the **monomer** in MeOD shows the successful addition of 1-amino-3,3-diethoxypropane to the **acid** product synthesized in the first step.

was successfully added. Furthermore, the presence of A, B, and C protons further suggest that the acetal linker was successfully added.

Figure 7 shows the ^{13}C NMR of the monomer. Like the ^{1}H spectrum, the ^{13}C spectrum contains the methyl and methylene acetal peaks and peaks representing

carbon atoms A, B, and C – thereby supporting the findings from the ^{1}H that the monomer was successfully synthesized.

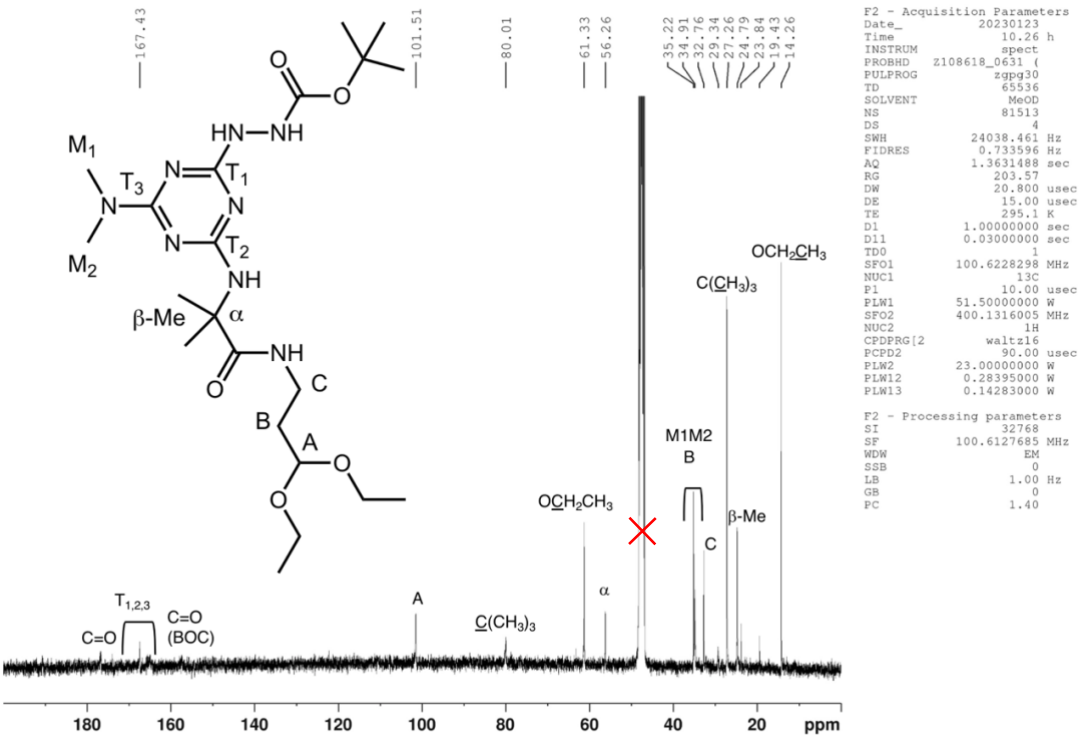

Figure 7**.** The ^{13}C NMR spectrum in MeOD shows the expected number of resonances and is consistent with the structure of the monomer intermediate.

Synthesis of ***AIB-AIB****.* The **monomer** was dissolved in a 1:1 solution of dichloromethane (DCM) and trifluoroacetic acid (TFA) and allowed to evaporate to dryness.

Silica gel exchange chromatography was performed to remove residual Hünig's base, consistent with the procedure described above regarding the purification of the acid intermediate.

Figure 8 shows the NMR spectrum of **AIB-AIB**. The position of the peak labeled A indicates that the cyclization occurred since the downfield shift of A between the monomer and macrocycle products shows that those protons are in different electronic environments. In the monomer, the A proton is located near two oxygen atoms, but in the macrocycle, the A proton is part of a hydrazone, which shifts the A protons downfield. Furthermore, the absence of the acetal resonances suggests that the linkage occurred.

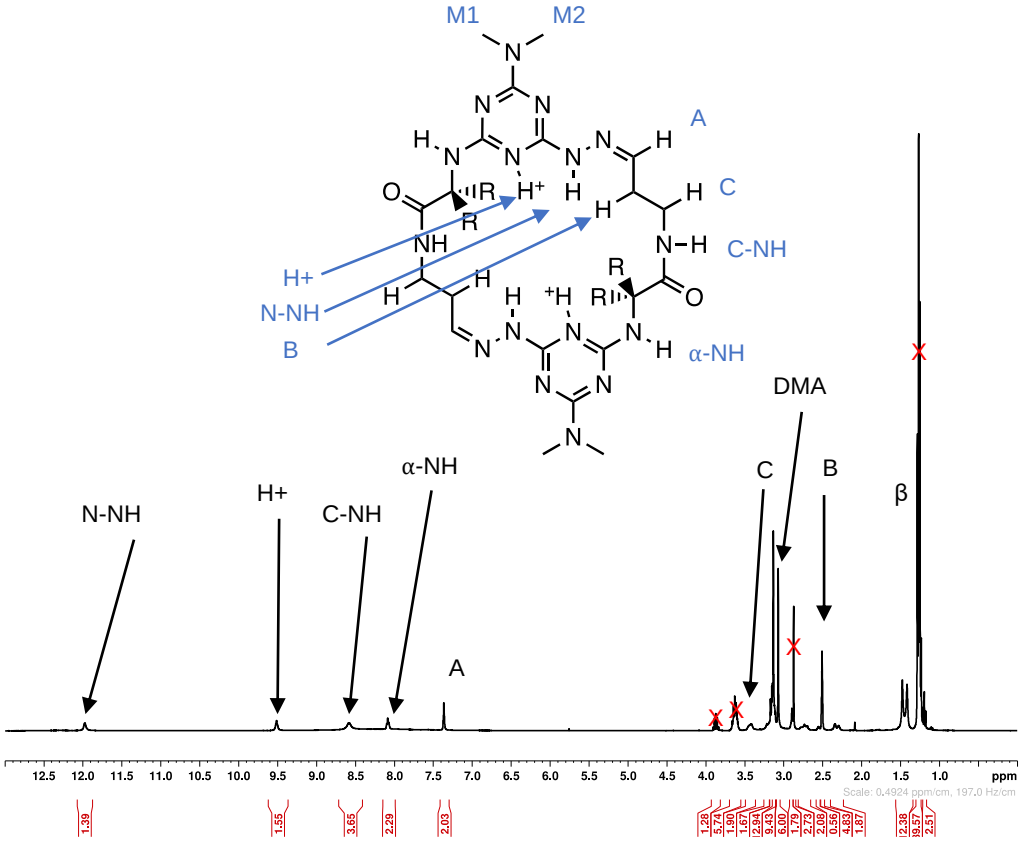

Figure 8. The ^{1}H NMR spectrum of the **AIB-AIB** macrocycle in DMSO-d_6. Labels depicted in blue assign the peaks in this spectrum to the protons on the molecule. The red "X" signifies an impurity in the spectrum and is not part of the **AIB-AIB** structure.

Figure 9 further supports the prediction that **AIB-AIB** formed. Again, the downfield shift of A and the absence of the acetal carbon further suggest that the macrocycle formed.

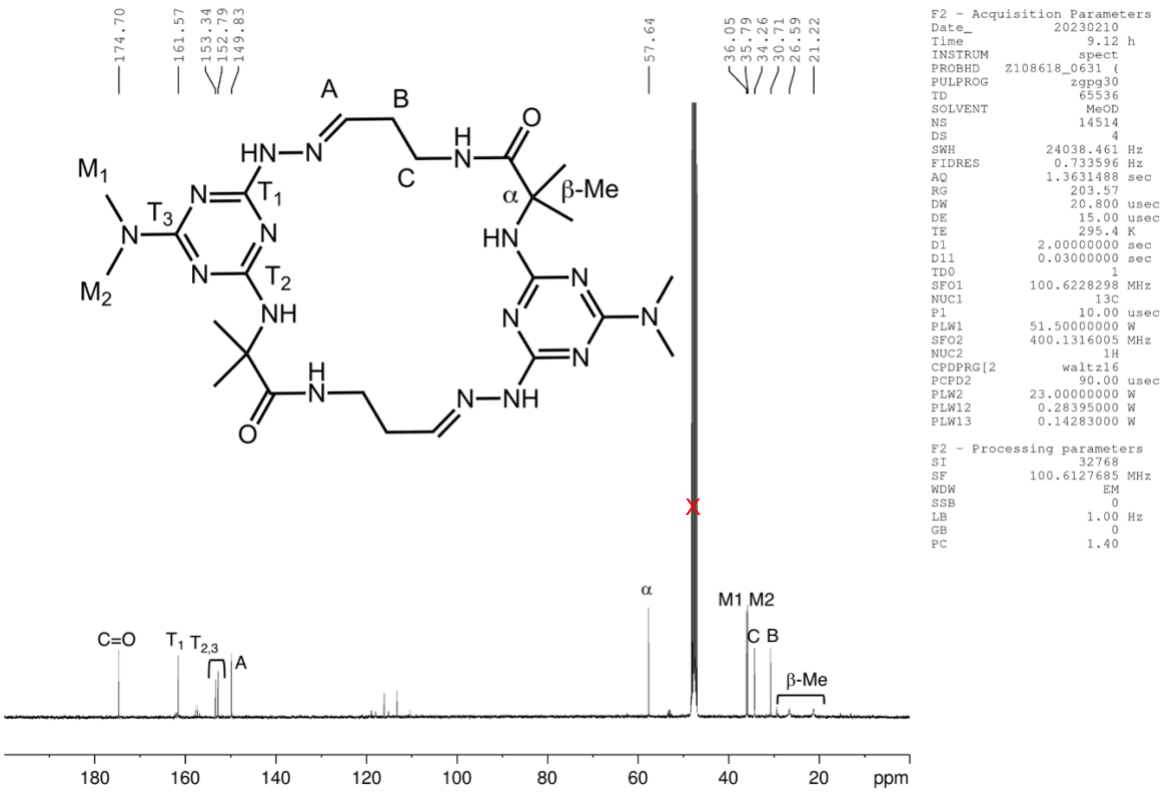

Figure 9. Carbon NMR Spectroscopy of **AIB-AIB** in CD_3OD

*Analysis of the 3-dimensional structure of **AIB-AIB**.* To determine the 3-D structure, 2-D NMR experiments were performed. A COSY experiment determined which atoms are near each other through bonds. A ROESY spectrum established 3-D structure. It does not determine how near atoms are through bonds but through space. Imagine that a large molecule is a trail around a lake with several hikers on the trail spaced out in regular increments. The COSY tells scientists which hiker is the closest by staying on the trail, but the ROESY tells scientists how far any two hikers are from each other as the

crow flies, which can include across the lake. Instead of hikers, chemists rely on the distance between hydrogen atoms to determine the molecule's structure.

Figure 10 shows the ROESY spectrum of **AIB-AIB**. The circled correlations on the ROESY spectrum indicate essential structural information. The rightmost point indicates that the protons on carbon A can see the protons on DMA, suggesting that the molecule must be folded so that those protons can "see" each other across the lake to reuse the above analogy. The second point shows that the proton on A and the N-NH proton can "see" each other. Because the protons can "see" each other, the A proton must be on the same side of the molecule as the N-NH proton, making the *E*-hydrazone configuration. If the N-NH and A protons could not see each other, the hydrazone would likely be in the *Z*-configuration. Chemists can use this structural naming scheme to indicate how groups orient across a double bond. *E* stands for entgegen, which is German for against, and *Z* stands for zusammen which is German for together.

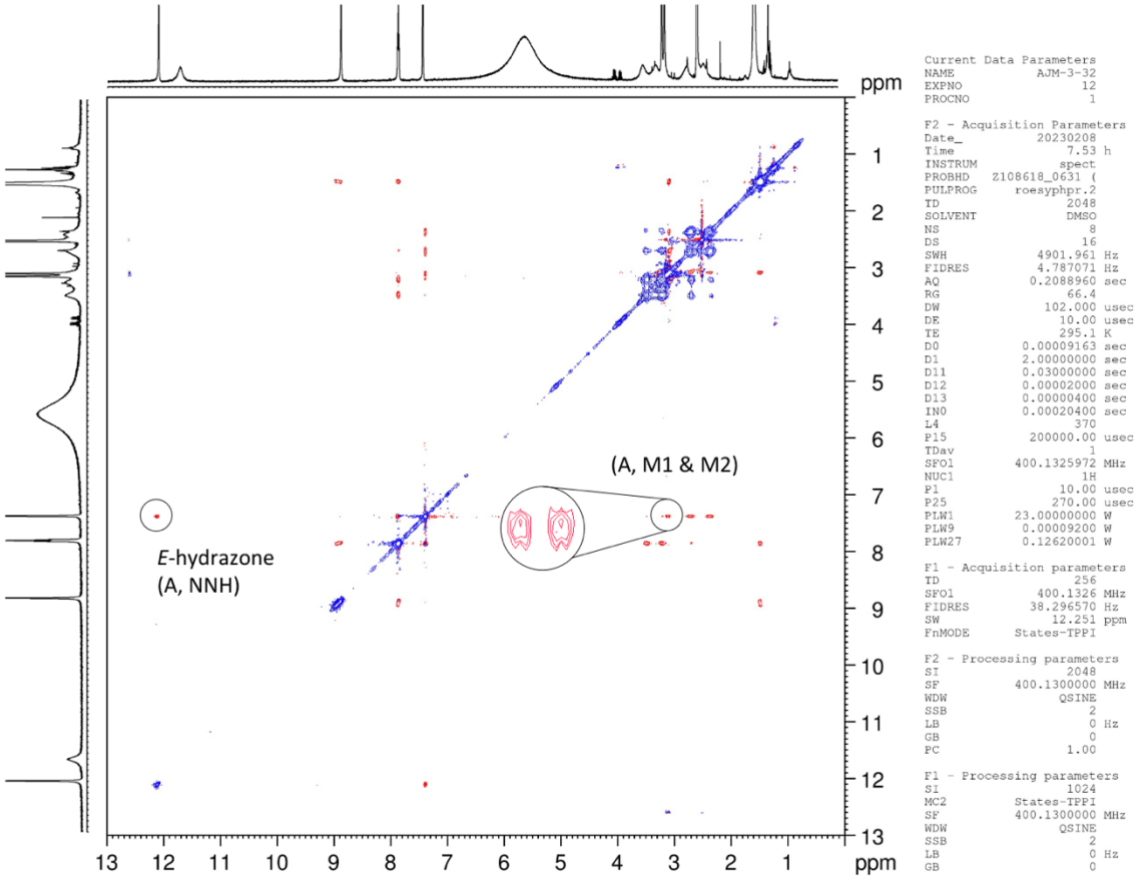

Figure 10. ROESY spectrum of **AIB-AIB** in DMSO-d_6

The picture that emerges from these data is a 3-D structure. Before discussing the solution conformation of the molecule, it is best to start with the solid-state structure. **Figure 11** shows how AIB-AIB folds in the solid state, which is identical to the shape it adopts in the solution based on the NMR spectra discussed above. In the case of the **AIB-AIB** macrocycle, the shape observed using XRD is the closed hinge conformation, with

the two aromatic rings offset from each other (**Figure 11**). This conformation is likely the most stable due to pi-pi stacking, wherein two aromatic systems near each other in space can stabilize each other – a feature that is also readily observed in deoxyribose nucleic acid (DNA). That conformation also minimizes ring strain, making it more favorable.

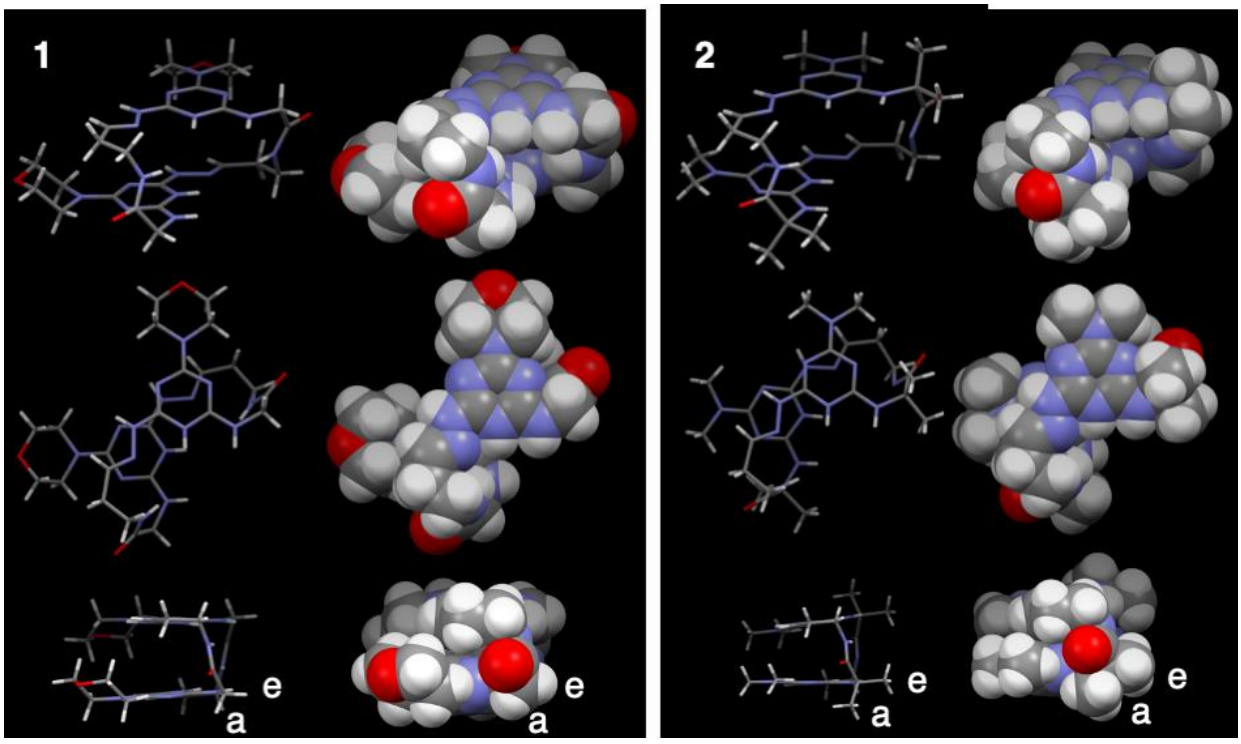

Figure 11. X-ray diffraction crystallography shows the structures of **G-G** (1) and **AIB-AIB** (2). One group varies. In **AIB-AIB**, the triazine has DMA. In **G-G**, the triazine has a morpholine ring. Aside from this difference, the structures are largely identical.

*Crystal structure of **AIB-AIB**.* Because the molecules of interest in this project are too small to be observed with the naked eye or with visible light microscopes, other methods must be used. One such method involves a technique called x-ray crystallography, or XRD. This technique takes advantage of the unique diffraction pattern that x-rays make when the x-rays hit an atom. A computer can analyze this diffraction

pattern to determine the structure of a molecule, which allows the static shape of the molecule to be readily determined.

*Mass spectroscopy of **AIB-AIB***. Another technique that can be used to determine the identity of a given compound is mass spectroscopy. In mass spectroscopy, the instrument ionizes a small amount of the sample and propels the sample through a tube using a magnetic field. Due to mass differences, molecules will separate themselves according to a mass-to-charge ratio. By analyzing these data, scientists can again determine if the target molecule has been synthesized. Scientists do this by using the periodic table to estimate how massive a target molecule should be. Then, by comparing the mass of the target molecule to the mass of the sample molecule, scientists can determine if the sample molecule is the target molecule. The three peaks in **Figure 12** on this spectrum result from the three isotopes of carbon in this sample: 12, 13, and 14.

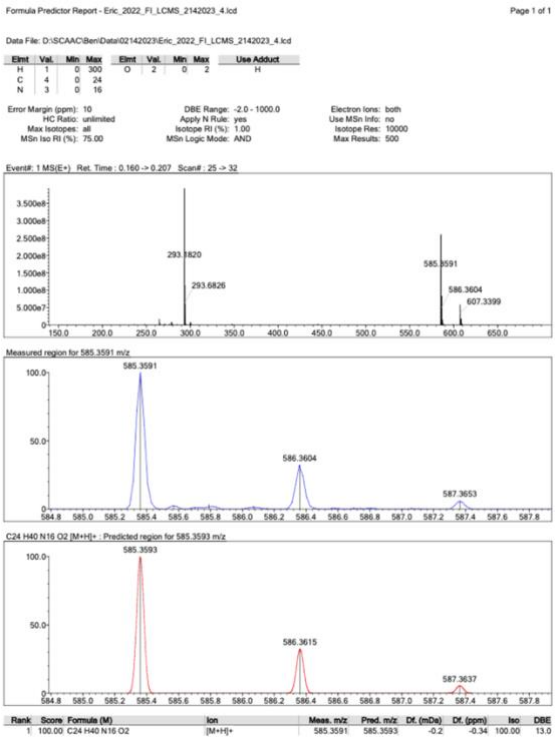

Figure 12. The mass spectrum of **AIB-AIB** is consistent with the predicted mass for this molecule.

Probing for hinge motion. The abovementioned techniques work exceptionally well for characterizing molecules that move randomly in solution, which covers most molecules. However, if the molecules behave in an ordered manner, then that motion can be further characterized using a few different techniques. The first technique of interest is variable temperature nuclear magnetic resonance spectroscopy (VT NMR). The NMR spectrum of a molecule shows its average structure. By analogy, a blur of the closed and open hinge. As temperature is lowered, then specific conformations can be observed. We observe the closed hinge conformation because the protons labeled “a” and “e” in **Figure 11** do not switch positions at low temperature. These protons are labeled “C” in **Figure 13** (blue dots). The same behavior is seen for the B protons (green dots) and the *β*-methyls of **AIB-AIB** (red dots).

In the case of the **AIB-AIB** macrocycle, four types of proton reach a coalescence

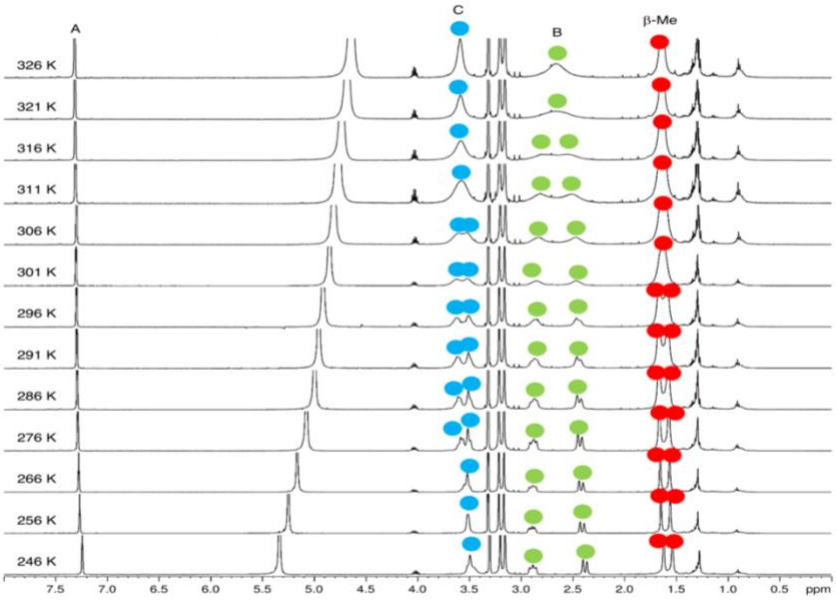

Figure 13. VT NMR in CD_3OD shows the coalescence of the β-Me (red), C (blue), and B (green) protons.

temperature. Those peaks are β-Me, B, DMA, and C. An important kinematic variable, k_{exch}, is the rate at which protons exchange (or change environments) can be calculated

using Equation 1**,** where $\Delta\boldsymbol{\nu}$ is the maximum difference in peak frequencies (ppm) when both resonances are fully resolved.

$$k_{exch} = \frac{\pi\Delta\nu}{\sqrt{2}} \qquad \textit{Equation 1}$$

This equation indicates that the protons at each position of interest are moving at different rates compared to each other. However, this is not the case since all protons of the hinge will exchange at nearly the same rate. Instead, this feature is due to the different coalescence temperatures. Because the protons with lower coalescence temperatures have the smallest $\Delta\boldsymbol{\nu}$, they will have the lowest proton exchange rate; but in reality, this number reports the hinging rate at a the coalescence temperature for that proton.

*Table 1. The NMR data for **G-G** and **AIB-AIB** in different solvents.*

Hinge	Solvent	Res.	v1	v2	Dv	$K_{exch.}$ sec^{-1}	T_c (K)
G-G	DMSO-*d*$_6$	a	—	—	—	—	—
		C	—	—	—	—	—
	MeOD-*d*$_4$	a	3.93	3.81	0.12	295	438
		B	2.77	2.43	0.33	108	264
	MeCN-*d*$_3$	a	4.31	3.01	1.30	100	258
		C	4.01	3.90	0.11	1157	274
	D_2O	a	—	—	—	—	—
		C	—	—	—	—	—
AIB-	DMSO-*d*$_6$	C	3.48	3.22	0.26	228	315

AIB		B	2.71	2.39	0.32	284	317
		b-Me	—	—	—	—	—
	MeOD-d_4	C	3.64	3.53	0.12	105	308
		B	2.86	2.49	0.37	324	316
		b-Me	—	—	—	—	—
	MeCN-d_3	C	4.08	3.24	0.84	1306	326
		B	2.78	2.57	0.21	190	311
		b-Me	1.72	1.62	0.10	92	304
	D_2O	C	3.48	3.44	0.04	34	308
		B	2.73	2.43	0.30	267	331
		b-Me	1.55	1.48	0.06	58	320

The most exciting observation in proton exchange rates is comparing the **AIB-AIB** and **G-G** macrocycles. The only structural difference between the two macrocycles is that the protons on the α position of the glycine amino acid are substituted for methyl groups, but the difference between these two macrocycles kinetically is profound. When compared in the same solvent, the **AIB-AIB** macrocycle exhibits this hinging motion at a significantly slower rate when compared to the **G-G** macrocycle. Clearly, the methyl groups are exerting an effect on the kinetics of these large molecules. In fact, these differences likely come down to a feature of molecules called sterics.

Sterics describe the repulsion between given atoms. Bonds exist in a sweet spot where overlap (stabilizing interactions) is maximized with respect to the repulsion (destabilizing interactions) exerted on each other. This repulsion is due to the electrons

(negatively charged subatomic particles) that want to repel each other like two opposing ends of a magnet with increasing force as they are brought closer together. This same effect occurs in molecules and is used to explain bond lengths and how favorable a given motion is. In the case of the **AIB-AIB** macrocycle, the methyl groups on the α position have to move nearby other atoms, and these other molecules, in turn, push back on that motion, thereby slowing the hinging motion down.

On the other hand, the **G-G** macrocycle has significantly smaller protons instead of bulkier methyl groups in the same position. These protons can more easily slide past each other as the hinging motion occurs, increasing the rate at which the hinging motion can occur.

The differences in hinging rate can be further quantified using Eyring's equation (see **Equation 2**), which relates coalescence temperature with important thermodynamic variables such as activation energy.

$$\Delta G^{\ddagger} = -ln\frac{hk_{exch}}{k_B T_c} * RT_c \qquad \textit{Equation 2}$$

The activation energy ($\Delta G^{\ddagger}$) measures how much energy is required to make a given reaction occur. Another term, enthalpy (ΔH), measures how much heat is either gained or lost in a given reaction, and entropy (ΔS) measures disorder in the system. Put together, these thermodynamic variables allow for a given movement to be quantified and thereby compared with movements observed in other molecules.

The use of Eyring's equation would produce intriguing data regarding the thermodynamics of this hinge motion. However, as of this writing, the data are not resolved well enough to allow meaningful conclusions to be gleaned.

CONCLUSIONS AND FUTURE

This work shows that a three-step process can successfully and efficiently synthesize the **AIB-AIB** macrocycle. Further, this molecule can be characterized using various techniques to determine its structure and movements. These characterization experiments show that steric congestion allows for control of the hinging motion and that the rate of the hinging motion can be changed depending on the solvent and temperature. Finally, future work on this project likely includes the measurement of logP and other biological properties to determine how this kinetic movement can impact bonding to important intracellular factors, which could lead to future therapeutic uses.

EXPERIMENTAL

NMR Spectroscopy. NMR spectra were recorded using a Bruker 400MHz Avance spectrometer. Chemical shifts in NMR experiments were referenced using a TMS standard present in each NMR solvent.

General Chemistry. Ion exchange chromatography experiments were performed using silica gel (Silicycle) with a porosity of 60 Å, a particle size of 50-63 µm, a surface area of 500-600 m^2/g, a bulk density of 0.4 g/mL, and a pH range of 6.5-7.5. A dichloromethane/methanol solvent system in various ratios was used as the eluent for

chromatographic purification. Thin-layer chromatography (TLC) experiments were performed using a dichloromethane/methanol solvent system in various ratios as the eluent and then visualized using a short-wave UV lamp and by treating with ninhydrin stain (1.5 g ninhydrin in 100 mL of n-butanol and 3.0 mL acetic acid) and heating using a heat gun. Excess solvents were removed using ambient or rotary evaporation on a Buchi Rotovapor RII with a Welch Self-Cleaning Dry Vacuum System. All procedures, including purification, were performed in ambient environmental conditions using reagent-grade solvents.

*Macrocycle **AIB-AIB**.* Fractions 11-14 from the Monomer AIB fraction were cyclized by adding 1 mL DCM to each fraction followed quickly by the addition of 1 mL neat TFA (trifluoroacetic acid). The fractions were allowed to stir and evaporate at room conditions for four weeks or until completely dry. Once the fractions evaporated, fractions 11-13 were combined and column chromatography was performed in a 19:1 solvent system to remove excess DIPEA. After fraction 11, the eluent system was switched to 9:1 DCM:MeOH to promote elution. A TLC of each fraction was performed, which showed little UV absorbance, but after drying, fraction 13 showed the most absorbance. Fraction 13 was then analyzed using proton NMR, which showed complete cyclization free from DIPEA contaminant thereby concluding this experiment. ^{1}H NMR (*DMSO-d_6*, 400MHz) δ 11.98 (s, 1H), 9.51 (s, 1H), 8.58 (s, 3H), 8.08 (s, 2H), 7.36 (s, 2H), 3.87 (5, 1H), 3.63 (m, 5H), 3.42 (m, 1H), 3.2170 (m, 1H), 3.13 (m, 12H), 3.07 (s, 6H), 2.90 (s, 1H), 2.87 (s, 2H), 2.32 (m, 1H), 1.45 (m, 12H), 1.27 (t, 39H), 1.19 (t, 2H)

*Monomer **AIB**.* This second step began with the addition of HOBT (93.5 mg, 0.692 mmol), HBTU (255.2 mg, 0.6729 mmol), DIPEA (180.0 mg, 1.222 mmol), 7 mL DMF and the DMA AIB Acid Intermediate 1 (209.0 mg, 0.588 mmol). This solution was allowed to stir for 1 hour before 3,3-diethoxypropylamine (92.5 mg, 0.628 mmol) was added and allowed to react overnight. The next day, a TLC of the reaction in 9:1 DCM:MeOH was performed resulting in the formation of new spots at rf 0.9, 0.8, 0.7 and 0.3. Silica gel exchange column chromatography was performed in a 39:1 DCM:MeOH eluent. Fraction 15 shows two spots at 0.7 and at the baseline. This fraction was analyzed by proton NMR and showed high concentrations of residual DIPEA but confirmed that the product successfully formed. Fractions 11-14 were a single, yellow spot with a small shadow at rf 0.8. The yellow spot was consistent with the spot analyzed by proton NMR and therefore suggested that these spots were the Monomer AIB. ^{1}H NMR (*Methanol-d_4*, 400 MHz) δ 5.51 (s, 1H), 4.49 (s, 5H), 4.66 (t, 1H), 3.72 (m, 3H), 3.57 (m, 3H), 3.33 (m, 6H), 3.00 (s, 13H), 1.95 (m, 3H), 1.51 (m, 2H), 1.22 (t, 8H)

*Intermediate **1**.* Cyanuric chloride (17.9508 g, 136.87 mmol) was added to 250 mL THF (tetrahydrofuran) and allowed to cool to -10˚C using an acetone/ice bath. Next, a solution of tert-butyl carbamate (Boc) (12.9508 g, 98.936 mmol) in 250 mL THF. The solution containing Boc was added to the first solution dropwise over 4 hours and 35 minutes using an addition funnel. The reaction showed a single spot by TLC with a faint streak, indicating that the reaction went to completion. Next, 25 mL of 5 N NaOH was added dropwise at a rate of 1 drop per second until the pH of the solution was 6. This intermediate is referred to as DCT, which stands for dichlorotriazine since only a single

chlorine has been replaced. Next, a solution AIB (10.0070 g, 97.04 mmol) in 485 mL water was prepared and stirred until the AIB had completely dissolved before it was added dropwise by addition funnel over 2 hours and showed 2 spots at rf 0.5 and 0.8 in 9:1 DCM:MeOH by TLC. Once this solution finished adding, 25 mL of 5 N NaOH was added over 15 minutes, which raised the pH from 4 to 8. Another TLC experiment was performed and showed the same spots present before the NaOH was added at 0.5 and 0.8. The reaction was allowed to continue stirring for another 3.5 hours and another TLC experiment was performed using an aliquot from 1.5 hours post addition and 3.5 hours post addition each showed one spot by TLC at 0.5 in 9:1 DCM:MeOH. The reaction mixture was allowed to stir overnight in a 40 ˚C water bath to complete addition. The next day, another TLC experiment was performed in 19:1 DCM:MeOH which showed the presence of three spots; two of which were yellow by ninhydrin stain at rf 0.5 and 0.2 and a red spot at the baseline. Next, this intermediate, called the MCT (monochlorotriazine) was extracted and washed with ethyl acetate. First, 10 mL of the reaction mixture at pH 6 was added to a separatory funnel and washed 3 times with 10 mL ethyl acetate. The TLC of the organic layer showed 4 yellow spots at rf 0.9, 0.8, 0.5 and 0.4; the aqueous layer had faint spots at rf 0.9, 0.8 and a streak from 0.5 to 0.4. The MCT product was analyzed using proton and carbon NMR, which confirmed that the addition was successful. Next, 250 mL,10 g of the MCT was removed from the reaction mixture and the solvent was evaporated using a rotary evaporator. Then silica gel exchange chromatography was performed on this sample. The chromatography was performed in a 9:1 DCM:MeOH eluent and the sample was dry-loaded onto the silica. To dry-load the product on the silica, 9:1 DCM:MeOH was added until the product dissolved, then 10 g of

silica gel was added and then the solvent was evaporated off using a rotary evaporator. This loaded silica was added to the top of the column and the chromatography was performed in 3% MeOH:DCM. After fraction 21, no product had eluted, so 30 mL of neat MeOH was added to 500mL 3% MeOH:DCM solution and added to the column. At fraction 30, 500 mL of 9:1 DCM:MeOH was added to the column and at fraction 34, 250 mL of 4:1 DCM:MeOH was added and allowed to elute into a 1 L Erlenmeyer. The next day, the liquid in the Erlenmeyer was colorless, which suggested that the product was still on the column, so 250 mL of 4:1 DCM:MeOH and 2 mL of ammonium hydroxide were added and allowed to elute into a 500 mL round bottom flask (RBF). Next, a TLC was performed. The solution from the round bottom flask had a single spot at rf 0.4 and was analyzed by proton and carbon NMR, which showed a single product. Another 250 mL of MeOH and 2 mL of acetic acid was added to the column and was allowed to elute into another round bottom flask, which showed 4 spots by TLC at rf 0.8, a steak from 0.6 to 0.2, 0.2 and baseline. Next, the pure MCT was rotovapped yielding 100 mg MCT. Then this final elution of the first column was dissolved in 50 mL of 9:1 DCM:MeOH and everything that dissolved was columned in 9:1 DCM:MeOH. The product from the Erlenmeyer from the first column was also rotovapped, yielding 2.299 g of product and column chromatography was again performed in 19:1 DCM:MeOH, and fraction 20 from this column was selected as the most pure and was combined with the pure MCT from the first column, which yielded 0.485 g, 1.40 mmol. This sample was split into one RBF for morpholine and a second for DMA addition. The morpholine flask contained 0.180 g, 0.5191 mmol MCT and the DMA flask contained 0.305 g, 0.8796 mmol. To the morpholine flask, 4 mL THF was added and allowed to dissolve the MCT. Next, morpholine was added rapidly at room

temperature (85.6 mg, 0.983 mmol). To the DMA flask, 2 mL of THF was added and allowed to dissolve the MCT before DMA was added (48 mg, 1.06 mmol) The acid intermediate was purified using silica gel exchange chromatography. Both reactions were allowed to complete overnight, and the next day TLC was performed in 9:1 DCM:MeOH which resulted in 2 spots at rf 0.5 and 0.4 with a shadow above 0.5 in morpholine and 1 spot at rf 0.3 for the DMA reaction. The TLC indicates that the morpholine addition was likely not complete, which was expected since the reaction was allowed to evaporate to dryness overnight. Next, 10 mL of water was added to the DMA solution and the pH was measured at 4. The DMA solution was then extracted and washed 3 times with 15 mL ethyl acetate. The organic layer was allowed to evaporate overnight and proton NMR the next day showed that DMA had not successfully added to the triazine ring in the DMA reaction. The morpholine solution was also checked by TLC and showed two spots at rf 0.7 and 0.4, suggesting that the morpholine reaction was not complete. Then, 4 mL THF was added to dissolve the morpholine precipitate and 2 mL of 1 N NaOH was added to bring the pH from 4 to 9. Then, 1 mL of additional DMA and morpholine were added to the DMA and morpholine reaction flasks respectively. The next day, both the DMA and morpholine acid intermediates were extracted using ethyl acetate. During the morpholine acid extraction, a colorless film appeared and was added to the organic layer. After the DMA extraction completed, the DMA acid was rotovapped down (209 mg, 0.588 mmol) and a proton NMR experiment was run which showed the complete addition of DMA onto the ring. The morpholine acid intermediate was later analyzed by proton NMR and did not show promising product formation. The gel (Silicycle) had a porosity of 60 Å, a particle size of 50-63 µm, a surface area of 500-600 m^2/g, a bulk density of 0.4 g/mL, and a pH

range of 6.5-7.5. A dichloromethane/methanol solvent system in a 19:1 ratio was used as the eluent for chromatographic purification.^{1}H NMR (*Methanol-d*$_4$, 400 MHz) δ 4.87 (s, 8H), 3.33 (5, 6H), 2.03 (s, 1H), 1.62 (s, 1H), 1.58 (d, 2H), 1.50 (s, 4H), 1.26 (t, 0.7155)

ACKNOWLEDGEMENTS

I would like to sincerely thank Dr. Simanek, the Simanek Research Group, and Drs. Minter and Stewart for their support and guidance throughout this project. I'd also like to thank the Robert A. Welch Foundation, the National Institutes of Health and the TCU Science and Engineering Research Center for supporting this research.